Asian Journal of Mycology 9(2): 513–530 (2026) ISSN 2651-1339
www.asianjournalofmycology.org

Article
Doi 10.5943/ajom/9/2/13

Cultivation, nutritional composition, and anticancer activity of ergosterol from the edible mushroom *Hericium coralloides* in Thailand

Gonkhom D[1,2], Aluksanasuwan S[3,4], Luangharn T[2], Hyde KD[2], Ebada SS[5,6], Somsuan K[3,4], Morchang A[3,4*] and Thongklang N[1,2*]

[1]School of Science, Mae Fah Luang University, Chiang Rai 57100, Thailand
[2]Center of Excellence in Fungal Research, Mae Fah Luang University, Chiang Rai 57100, Thailand
[3]School of Medicine, Mae Fah Luang University, Chiang Rai 57100, Thailand
[4]Cancer and Immunology Research Center (CIRC), Mae Fah Luang University, Chiang Rai 57100, Thailand
[5]Department of Microbial Drugs, Helmholtz Centre for Infection Research (HZI), and German Centre for Infection Research (DZIF), partner site Hannover/Braunschweig, Inhoffenstrasse 7, 38124 Braunschweig, Germany
[6]Department of Pharmacognosy, Faculty of Pharmacy, Ain Shams University, Organization of African Unity Street 1, P.O. 11566 Cairo, Egypt

Gonkhom D, Aluksanasuwan S, Luangharn T, Hyde KD, Ebada SS, Somsuan K, Morchang A, Thongklang N. 2026 – Cultivation, nutritional composition, and anticancer activity of ergosterol from the edible mushroom *Hericium coralloides* in Thailand. Asian Journal of Mycology 9(2), 513–530, Doi 10.5943/ajom/9/2/13

Abstract

Hericium coralloides is a remarkable mushroom valued for both culinary applications and potential health benefits. This study represents its first successful cultivation in Thailand using locally available agricultural substrates. *Hericium coralloides* strain STMA 14278, obtained from Germany, was cultivated on three different substrate treatments. Fresh fruiting bodies were harvested, dried into powder form, and subjected to proximate analysis to determine the nutrient composition. For chemical profiling, the dried mushroom powder was extracted using ethyl acetate, followed by fractionation and purification through silica gel column chromatography. The isolated compounds were identified through thin-layer chromatography and $^{1}H/^{13}C$ nuclear magnetic resonance (NMR) spectroscopy. Three isolated compounds were identified as (22*E*)-ergosta-7,9,22-trien-3*β*-ol (1), hericene A (2), and ergosterol (3). The anticancer potential of the isolated compounds was evaluated against A549, SW-480, and Huh-7 cancer cell lines using 3-(4,5-dimethylthiazol-2-yl)-2,5-diphenyltetrazolium bromide (MTT), clonogenic, and apoptosis assays. The results revealed successful fruiting body formation across all three substrates, yielding 141.40, 138.20, and 142.50 g per cultivation bag, respectively. Proximate analysis of the dried mushroom powder revealed a protein content of 18.81 g/100 g. Three compounds were purified from the fruiting bodies, with ergosterol exhibiting the most potent cytotoxicity against cancer cells. The IC_{50} values of ergosterol were 4.6, 5.2, and 4.2 µg/mL against A549, SW-480, and Huh-7 cells, respectively. Additionally, ergosterol treatment significantly inhibited colony formation and cell migration in A549, SW-480, and Huh-7 cell lines. In conclusion, *H. coralloides* represents a promising source of bioactive compounds with potential anticancer properties. The isolated ergosterol exhibits significant cytotoxicity against cancer cells, highlighting its potential for further investigation as a therapeutic agent.

Submitted 19 September 2025, Accepted 19 June 2026, Published 3 November 2026
Corresponding Author: Atthapan Morchang – e-mail – atthapan.mor@mfu.ac.th;
Naritsada Thongklang – e-mail – naritsada.t@gmail.com

Keywords – anticancer – coral tooth fungus – cultivation – ergosterol – silica gel column

Introduction

Hericium coralloides, a species in the family Hericiaceae, is commonly known as the coral mushroom, coral tooth fungus, or coral hedgehog (Shrivastava & Jain 2024). It is characterized by its distinctive cascading spines that resemble coral formations (Van der Merwe et al. 2023) and typically grows on hardwoods in natural environments (Shrivastava & Jain 2024). *Hericium coralloides* has also been referred to by several synonyms, including *H. abietinum*, *H. ramosum*, and *H. reichii* (Shrivastava & Jain 2024, Index Fungorum 2026). This species is relatively rare and has been reported primarily in parts of Europe and Asia (Shrivastava & Jain 2024).

Hericium coralloides is a well-known edible mushroom valued for its distinctive flavor and both culinary and medicinal properties (Demirtas et al. 2024, Shrivastava & Jain 2024). Its delicate taste is often compared to seafood, such as crab or lobster (Sholyavei et al. 2020). This mushroom is rich in macronutrients and B vitamins, including thiamine (B1), riboflavin (B2), niacin (B3), and pantothenic acid (B5) (Sostherb 2023). Furthermore, it contains essential minerals such as potassium, zinc, iron, and selenium (Heleno et al. 2015). These nutritional attributes contribute to its value as a dietary component and support its potential therapeutic applications (Lazur et al. 2024).

Hericium coralloides is a fascinating medicinal mushroom with potential therapeutic benefits for various health conditions, including neuroprotection, anti-inflammatory and immune-boosting effects, as well as antioxidant, anti-aging, and anticancer properties (Thongbai et al. 2017, Zhang et al. 2019, Guan et al. 2023, Williams et al. 2023, Shrivastava & Jain 2024, Qi et al. 2025). This mushroom has gained increasing attention due to its extensive pharmacological effects on chronic illness, particularly for cancer prevention or as a complementary treatment (Qi et al. 2025).

Due to its beneficial properties, *Hericium coralloides* is an intriguing fungus for cultivation. Several *Hericium* species, particularly *H. erinaceus*, are commonly cultivated on sawdust-based substrates (Qi et al. 2025). While *H. erinaceus* is widely used in commercial cultivation, *H. coralloides* presents unique challenges and requires specific environmental conditions and cultivation techniques for successful growth. Substrate cost is a significant factor in mushroom cultivation; however, most commercial efforts have focused on *H. erinaceus* (Ko et al. 2005). Despite its therapeutic properties, the cultivation of *H. coralloides* remains limited, and to date, no studies have assessed the utilization of agricultural by-products as alternative substrates for its cultivation (Pasailiuk et al. 2019).

Although *Hericium* species have been cultivated in several countries, reports on the cultivation of *H. coralloides* remain limited, particularly in tropical regions (Thongbai et al. 2017). To our knowledge, there are no documented reports of the successful cultivation of *H. coralloides* in Thailand utilizing local agro-industrial waste. Developing cultivation strategies using regional agricultural residues not only supports sustainable mushroom production but also enhances the economic feasibility of functional mushroom cultivation (Miles & Chang 2004, Grimm & Wösten 2018).

Previous chemical investigations of *H. coralloides* have revealed a diverse array of metabolites, including sterols, terpenoids, and aromatic compounds with promising biological activities (Jianzhao et al. 2024). Among these, (22*E*)-ergosta-7,9,22-trien-3*β*-ol (**1**), a sterol derivative, has been reported in various fungi and is associated with antioxidant and anti-inflammatory effects. However, its anticancer activity remains underexplored (Chen et al. 2020, Qi et al. 2025). Hericene A (**2**), a triterpenoid unique to the genus *Hericium*, has been described for its neuroprotective and antiproliferative potential (Wittstein et al. 2016). Ergosterol (**3**), the most abundant fungal sterol, is widely recognized for its diverse pharmacological actions, including cytotoxic, anti-inflammatory, and anti-angiogenic effects across various cancer models (Lin et al. 2022, Rangsinth et al. 2023).

Currently, several cancer cell lines with high global incidence and mortality, including A549 (lung adenocarcinoma), Huh-7 (hepatocellular carcinoma), and SW-480 (colorectal adenocarcinoma) are widely used as models for anticancer screening (Bray et al. 2024, Wiraswati et al. 2025), and they are among the most prevalent cancers reported in Thailand. Due to their biological relevance, it is essential to preliminarily assess the potential of *H. coralloides*-derived compounds to inhibit proliferation, colony formation, and migration in these malignancies.

Therefore, this study aims to identify alternative, cost-efficient ingredients for sawdust-based substrates to support the cultivation of *H. coralloides*, and to analyze their nutritional composition. Furthermore, the isolated compounds from the cultivated mushrooms were evaluated for their nutritional, chemical profiling, and evaluation of their anticancer activity against selected cancer cell lines.

Materials & Methods

Mushroom strain and spawn preparation

A pure culture of *Hericium coralloides* (STMA 14278) was obtained from the Institute of Department Microbial Drugs, Helmholtz Centre for Infection Research (HZI), in Braunschweig, Germany. The strain was subcultured and maintained on potato dextrose agar (PDA) at 25 °C for 15 days, then stored at 4–7 ºC for up to three months for short-term preservation (Sinclair & Dhingra 2017, Thongbai et al. 2017). The mushroom grain spawn was prepared using red sorghum (*Sorghum bicolor* (L.) Moench) following the method described by Thongbai et al. (2017). The inoculated grains were incubated at room temperature (25 ± 2 °C) until the mycelium fully colonized the grain, after which it was used for cultivation.

Substrate treatments, preparations, and mushroom cultivation

Para rubber (*Hevea brasiliensis*) sawdust was used as the base material in the preparation of three different substrate treatments for cultivating *Hericium coralloides* (STMA 14278) (Table 1).

Table 1 Composition and ingredient costs of substrate treatments used for cultivating *Hericium coralloides* (STMA 14278).

Substrate	*Cost ($/kg)	Substrate Treatment (kg)		
		T1	T2	T3
Red sorghum	0.61	-	15	-
Gypsum ($CaSO_4 \cdot 2H_2O$)	3.00	-	1	0.4
Lime (CaO)	0.10	-	1	0.8
Magnesium sulfate ($MgSO_4$)	0.29	-	-	0.2
Molasses	0.25	-	1	-
Para rubber sawdust	0.15	95	77	88
Rice bran	0.04	3	3	9
Rice flour	0.35	-	-	0.8
Sugar	1.00	2	-	0.8
Yeast powder	36.00	-	2	-

Note: "-" indicates that the component was not included in the respective substrate treatment. * Cost of each of the additional ingredients from the Alibaba website (https://www.alibaba.com), accessed in October 2025.

After thoroughly mixing each substrate treatment, the moisture content was adjusted to approximately 70%. Six hundred grams of each substrate mixture were placed into polypropylene bags and sterilized at 121 °C under 15 psi pressure for 40 minutes. The sterilized bag was allowed to cool down before inoculation. Each cooled bag was inoculated with 3 grams of actively growing grain spawn and incubated in darkness at room temperature (25 ± 2 °C) for 40 days. The

experiment was conducted with five replications. Once full mycelial colonization was observed, the bags were opened under controlled conditions (18–20 °C and 90% relative humidity). Primordia formation was observed within 10–14 days, followed by the development of fruiting bodies in 21–24 days. Fruiting bodies were harvested at maturity and weighed to determine biomass production (Stamets 2011).

Evaluation of cultivation parameters

The fresh weight of the fruiting bodies from the first flush (grams), the time taken for the first flush (days), the number of flushes per bag (fruiting bodies), and the total yield of fruiting bodies (grams) for each substrate treatment was recorded (Stamets 2011). After harvesting, the weight of each fresh mushroom and the number of fruiting bodies per bag were recorded, and biological efficiency (BE%) was calculated (Stamets 2011). To determine dry weight, the fresh mushrooms were dried in a hot air oven at 45 °C for 48 hours (Pewlong et al. 2019).

Proximate composition analysis

Fruiting bodies were dried at 45 °C for 48 hours and subsequently ground into a powdered form using a blender. The mushroom powders were analyzed for ash, carbohydrates, crude fiber, energy, fat, moisture, and protein content. These parameters were determined according to AOAC guidelines and standard methods used for nutrition labeling analysis (AOAC 2019, AOAC 2023, FAO 2003), and details were described in Table 2.

Table 2 Proximate composition analysis method used to determine nutritional contents of dried *Hericium coralloides* fruiting bodies.

Proximate Composition	Analytical Methods
Ash	AOAC (2019) 923.03 and 920.153
Carbohydrate	AOAC (2023)
Crude fiber	AOAC (2019) 978.10
Energy	FAO (2003)
Fat	AOAC (2019) 948.15
Moisture	AOAC (2019) 925.10 and 950.46
Protein	AOAC (2019) 991.20

Statistical analysis of mushroom cultivation

Statistical analyses were performed using IBM SPSS Statistics version 2. A one-way analysis of variance (ANOVA) was used to evaluate the significant differences among the means of *Hericium coralloides* grown on three different substrate treatments. Mean comparisons were conducted using Duncan's multiple range tests at a 95% confidence level ($p < 0.05$).

Preparation of extracts

The 100 g of dried *Hericium coralloides* mushroom powders were refluxed with 95% acetone (1000 mL) and placed on a shaker at 120 rpm at room temperature (25 ± 2 °C) for 24 hr. After filtering the sample, 1000 mL of acetone was used twice to remove the residue. The collected filtrate was subsequently extracted using ethyl acetate according to the previously mentioned method (Wittstein et al. 2016) and dried under reduced pressure using a rotary evaporator. The following produced 15 grams of crude ethyl acetate extract.

Chromatographic separation

Thin-layer chromatography (TLC) was utilized after silica gel column chromatography to separate the dried extracts. For silica gel column chromatography, the dried extract was dissolved with two combinations of solvents. The ratios of two combinations of the solvents were EtOAc:*n*-hexane in 20:80 for the polarity to shift monotonically. The stationary phase of the silica gel

column was Kieselgel 60. Following the loading of the samples onto the silica gel column, the solvent was used to elute the column. The purification and isolation of compounds from *H. coralloides* workflow is provided in Supplementary Figure S1.

For an additional four products of secondary metabolites, the ethyl acetate extract was purified by chromatography on a silica gel column, using *n*-hexane gradient system: ethyl acetate (20:80) (R2), resulting in eleventh fractions, and fraction 5 (compound **1**) was collected for NMR analysis. After that, R2F3 (20% ethyl acetate:*n*-hexane) (R3) was further separated according to the previously mentioned method, resulting in ten fractions, and fraction 4 (compound **2**) was collected. Fraction 10 was used in the silica column with a solvent of 20% acetone:*n*-hexane (R4), resulting in nine fractions, collected fraction 1 (compound **1**). Fraction 4 was combined with fraction 6 (20% ethyl acetate:*n*-hexane) (R3) and was further separated according to the previously mentioned method, resulting in ten fractions and collected fraction 6 (compound **3**). All fractions were collected from the solvent. Chemical structures of the isolated compounds, **1** (R2F6 and R4F1), **2** (R3F4), and **3** (R5F6), were identified by correlating the experimental NMR data with the published values in previous studies.

Compound characterizations

Chemical structures of the isolated compounds were determined using spectroscopic techniques, with ^{1}H (500 MHz), and ^{13}C NMR (125 MHz) spectral data compared with previously published physical properties and NMR spectra.

Cell culture preparation

Human non-small cell lung cancer cells (A549; CCL-185, American Type Culture Collection (ATCC), Manassas, VA, USA), hepatocellular carcinoma cells (Huh-7; JCRB0403, Japanese Collection of Research Bioresources (JCRB), Osaka, Japan), and colorectal cancer cells (SW-480; CCL-228, ATCC) were maintained in Dulbecco's Modified Eagle Medium (DMEM, Gibco, Thermo Fisher Scientific, Waltham, MA, USA) containing 10% (v/v) fetal bovine serum (FBS; Gibco), 100 U/mL penicillin, and 100 µg/mL streptomycin (Gibco). The cells were incubated at 37 °C in a humidified atmosphere with 5% CO_2.

Preparation of *Hericium coralloides* extract for cell treatment

The isolated chemical compounds were purified from the fruiting bodies of *H. coralloides* cultivated at Mae Fah Luang University, Chiang Rai Province, Thailand. All compounds were solubilized in dimethyl sulfoxide (DMSO) and used for cell treatments.

MTT cytotoxicity assay

Cells were seeded in a 96-well plate at a density of 7×10^3 cells per well and incubated for 24 hours. The cells were then treated with different concentrations (0–50 µg/mL) of the compounds (**1**–**3**) and incubated for 72 hours. The MTT solution (0.5 mg/mL) was added to all wells and incubated for 2 hours at 37 °C. After removing the culture supernatant, DMSO was added to dissolve the dark blue crystals, and the solution was mixed thoroughly. The optical density was measured at 570 nm using a microplate reader (Tecan Austria GmbH, Grödig, Austria). The percentages of cell viability and IC_{50} values were calculated using GraphPad Prism (version 10.3; San Diego, CA, USA).

Clonogenic survival assay

A clonogenic assay was performed as previously described (Morchang et al. 2025). Cells were seeded in 96-well plates at a density of 7×10^3 cells per well and incubated for 24 hours. Afterwards, the cells were treated with each compound at concentrations of 0, 5, or 10 µg/mL for 24 hours. Following treatment, the cells were trypsinized, reseeded into 12-well plates at 1×10^3 cells per well, and cultured in a complete medium for 7 days. The attached cells were then fixed with cold absolute methanol for 15 minutes and stained with 0.5% (w/v) crystal violet at room

temperature overnight. Subsequently, excess crystal violet was washed off with tap water. The plates were air-dried and photographed using the ChemiDoc™ Touch Imaging System (Bio-Rad Laboratories, Hercules, CA, USA). The plates were added with 33 % acetic acid, incubated for another 10 min., and measured at 570 nm using a microplate reader (Tecan Austria GmbH, Grödig, Austria). The percentages of cell viability and IC_{50} values were calculated using GraphPad Prism (version 10.3; San Diego, CA, USA).

Wound healing-scratch assay

The effect of the compound on cell migration was examined using a wound healing-scratch assay, as previously described (Aluksanasuwan et al. 2024, Somsuan et al. 2025). A total of 2×10^5 cells were plated in 6-well plates and incubated overnight at 37 °C in a 5% CO_2 atmosphere. Once the cells reached 100% confluence, a 200 µL pipette tip was used to create a scratch on the monolayer cells at the bottom of each plate. The cell debris was then removed with PBS, and the remaining cells were cultured in a complete medium with each of the three isolated compounds at concentrations of 0, 5, and 10 µg/mL for 24 hours. Images of the gap area were captured at 0 hours and 24 hours post-scratching using, a Zeiss Primovert inverted microscope (Carl Zeiss Microscopy GmbH, Jena, Germany). The wound area was analyzed using Image J software with the wound healing size tool plugin (Suarez-Arnedo et al. 2020).

Results and Discussion

Fruiting body development and morphological characteristics of *Hericium coralloides*

Hericium coralloides (STMA 14278) successfully formed fruiting bodies on all three substrate treatments. Primordia formation was initiated within 14–18 days following the opening of cultivation bags containing fully colonized substrates, and the first flush of mature fruiting bodies developed within 21−28 days, with individual fruiting bodies exhibiting a fresh weight ranging from 43 to 87 grams. Pinhead development was observed at a temperature of 18−20 °C, followed by branching and expansion of the fruiting bodies at 20−24 °C under a relative humidity of 90−95%.

The development of fruiting body growth of *H. coralloides* is shown in Fig. 1. The morphological characteristics of *H. coralloides* were highly branched and with lengths ranging from approximately 2 to 10 cm. Their structure resembled coral formation or icicles, as previously described by Kuo (2020) and Zhu et al. (2024). The coloration ranged from white to cream, with occasional yellow or orange discoloration in mature specimens (Zhu et al. 2024). The fruiting bodies of *H. coralloides* produce a white to yellowish, slender, irregularly shaped branches bearing dense, hair-like, or thorn-like structures. The mature fruiting bodies measure approximately 4–11 cm in height, with a stipe diameter of 1–2 cm. These branches exhibit irregular forms due to environmental conditions that are suboptimal for the development of fruiting bodies, such as insufficient CO_2 levels, light, or air exchange, resulting in abnormal mushroom morphology compared to Zhu et al. (2024). The mature fruiting bodies grown on all growing substrates are shown in Fig. 2.

Among the three-substrate treatments, the fresh weight of *Hericium coralloides* fruiting bodies showed no significant differences and ranged from 43 to 87 g per 600 g of substrate. The total yield of *H. coralloides* (STMA 14278) across treatments ranged from 138 to 142 g/kg of substrate, with the biological efficiency (B.E.) varying between 18.43% and 19.00% (Table 3). These results revealed no statistically significant differences in yield among the three treatments ($p = 0.05$). These results are consistent with those reported by Ko (2005) and are higher than those reported by Atila (2021), who reported a yield of 101 g/kg for *H. coralloides*.

Although substrate treatment 2 (T2) contained a more complex formulation with additional nutrient supplements, statistical analysis revealed no significant differences in fresh weight, total yield, or biological efficiency (B.E.) among the three substrate treatments (T1–T3) (Table 3). All substrate treatments were based on para-rubber sawdust supplemented with various ingredients. T1

included rice bran and sugar. T2 was enriched with red sorghum, gypsum ($CaSO_4 \cdot 2H_2O$), lime (CaO), molasses, rice bran, and yeast powder. T3 contained gypsum ($CaSO_4 \cdot 2H_2O$), lime (CaO), magnesium sulfate ($MgSO_4$), molasses, rice bran, rice powder, and sugar.

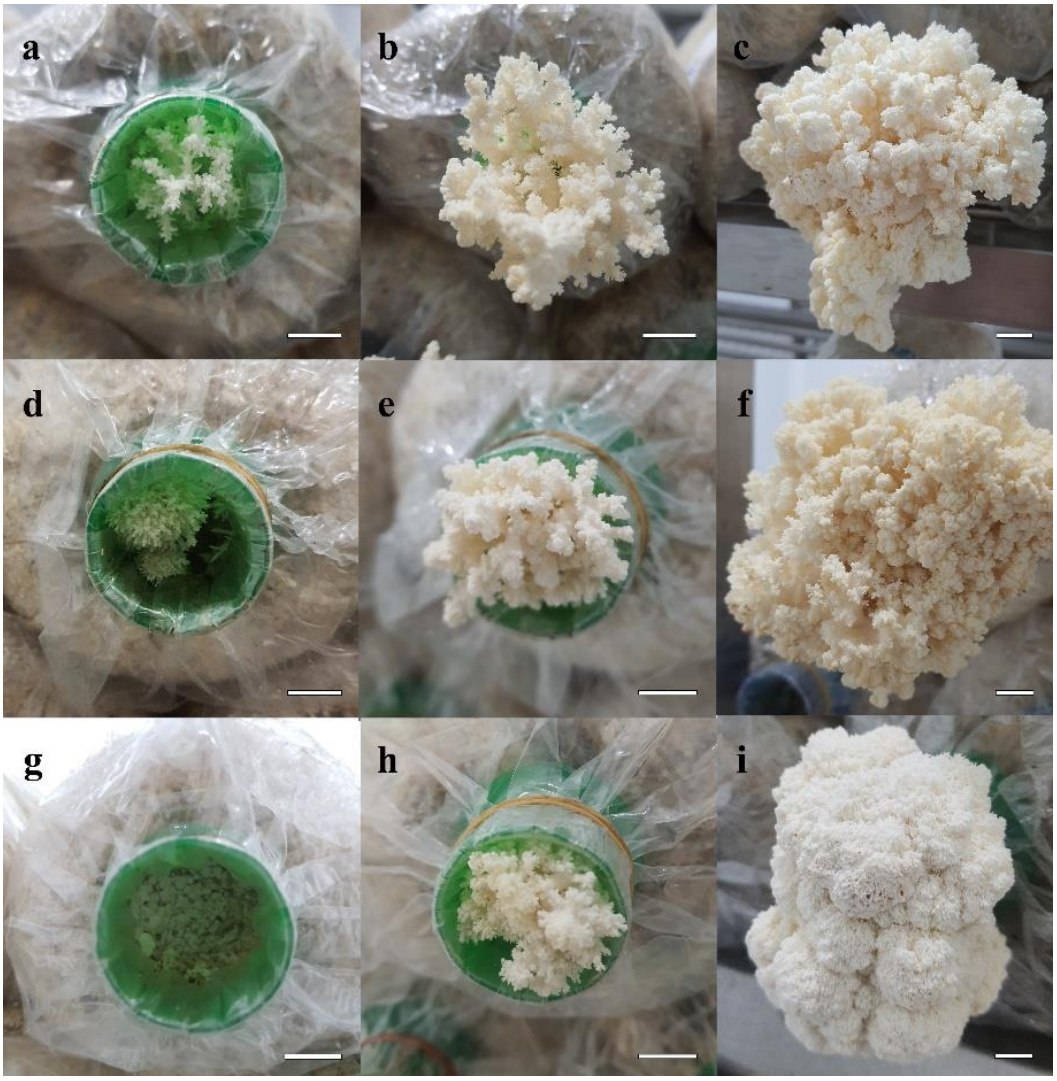


Fig. 1 – Developmental stages of fruiting body growth in *H. coralloides* (STMA 14278), showing pinhead formation (Days 14–18) and mature fruiting body development (Days 21–28). a–c *H. coralloides* cultivated on substrate treatment number 1. d–f *H. coralloides* growing on substrate treatment number 2. g–i *H. coralloides* growing on substrate treatment number 3. Scale bar = 1 cm.

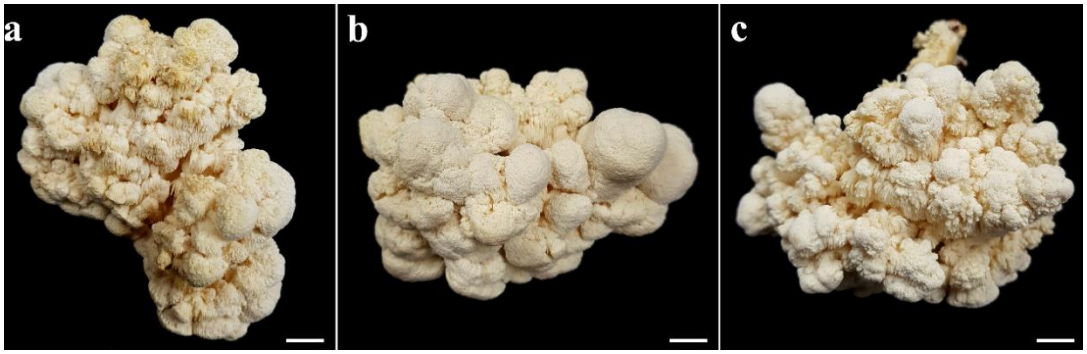


Fig. 2 – Mature fruiting bodies of the *H. coralloides* (STMA 14278). a–c Mature fruiting bodies from substrate treatment numbers 1−3, respectively. Scale bar = 1 cm.

The ingredient costs for each substrate treatment are detailed in Table 1. The ingredient costs for each T1, T2, and T3 were $16.37, $96.17, and $15.97, respectively. T3 achieved the highest B.E. (19.00%), while T1 provided a slightly lower yield but was significantly more cost-effective due to lower substrate expenses (USD 15.97 vs. 96.17 for T2). These findings indicate that *H. coralloides* can effectively utilize relatively simple substrates. This adaptability offers a significant advantage by reducing cultivation costs and enhancing the economic viability of commercial-scale production in Thailand.

Table 3 Comparison of the first flush yield and cultivation performance of *H. coralloides* (STMA 14278) grown on different substrate treatments.

Parameters	Substrate treatment 1	Substrate treatment 2	Substrate treatment 3
Fresh weight of fruiting bodies of flush 1 (g)	56.56 ± 11.67[a]	55.29 ± 11.21[a]	57.01± 17.95[a]
Time taken for flush 1 (days)*	38	38	40
Number of flushes	3	3	3
Total yield (g)	141.4	138.2	142.5
Biological Efficiency (%)	18.85 ± 3.9[a]	18.43 ± 3.7[a]	19.00 ± 5.9[a]

Note: * Period from the end of the incubation phase (full colonization) to the initiation of the first fruiting flush. Means within a row sharing a common superscript letter ([a]) do not differ significantly (p = 0.05, Duncan's Multiple Range Test).

Proximate composition of *Hericium coralloides*

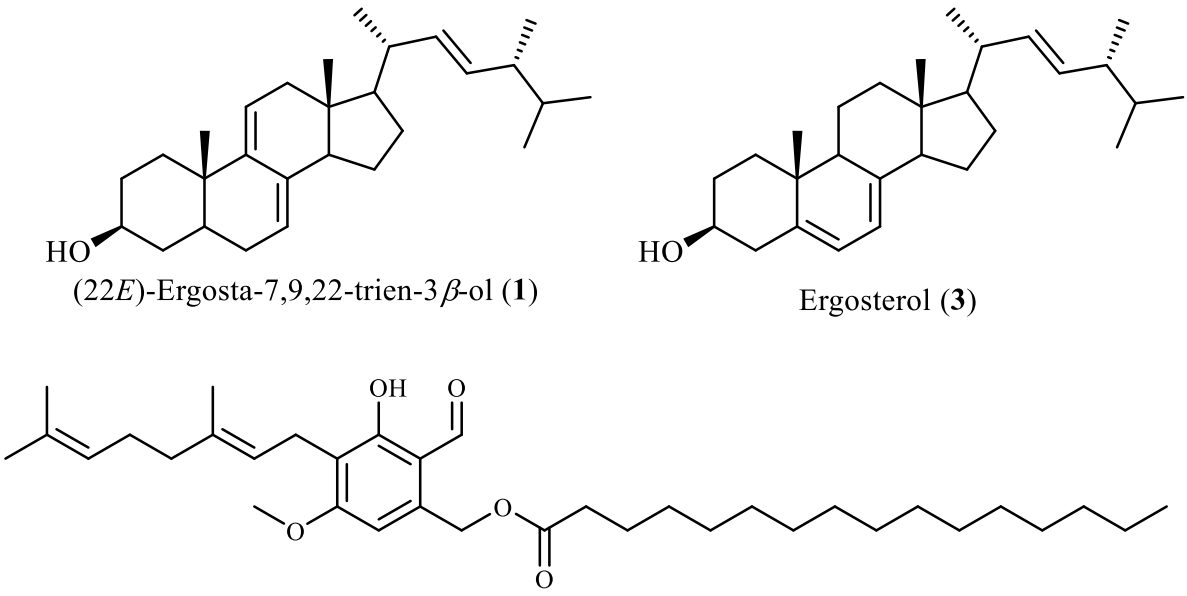
The proximate compositions of *H. coralloides* (STMA 14278) from the substrate treatment 2 were as follows: protein content 18.81%, crude fiber 4.61%, fat 6.43%, ash 13.88%, carbohydrate 49.98%, moisture 10.90%, and energy value 333.03 kcal per 100 g. The proximate composition values obtained in this study were broadly comparable to those previously reported for *Hericium* species, which also show similarities in ash, lipid, carbohydrate, crude fiber, elemental, and protein content (Atila et al. 2021, Gonkhom et al. 2024). Atila (2021) reported protein and ash contents of 17.4% and 8.5%, respectively, for *H. coralloides*. In comparison, the protein content observed in the present study (18.81%) was slightly higher, while the ash content (13.88%) was considerably higher. The elevated ash content may reflect a higher mineral accumulation in the fruiting bodies, which could be influenced by the mineral composition of the cultivation substrate, particularly the presence of gypsum, lime, and other mineral supplements used during cultivation (Miles & Chang 2004).

Identification of compounds

Hericium coralloides produces several phytochemical groups, such as polysaccharides, triterpenoids, phenolic compounds, sterols, fatty acids, amino acids, and other compounds (Jianzhao et al. 2024). Previous phytochemical investigations in *H. coralloides* have revealed the presence of alkaloids such as corallocins B−D (Wittstein et al. 2016), benzofurans such as corallocin A, hydrospirobenzofuran, spirobenzofuran, and sesquibenzopyran (Wittstein et al. 2016, Kim et al. 2018), phenols such as coralcuparene (Kim et al. 2018), sterols such as ergosterol (Lazur et al. 2024), terpenoids such as erinacine (Koga 2024), and polysaccharides (Zhang et al. 2024).

Three known compounds, (22*E*)-ergosta-7,9,22-trien-3*β*-ol (**1**), hericene A (**2**), and ergosterol (**3**) (Fig. 3), were isolated from 15 g of crude extract, yielding 35 mg (0.233%), 50 mg (0.333%), and 13 mg (0.087%), respectively. Relative to 100 g of dried mushroom, the isolated amounts corresponded to 0.035%, 0.050%, and 0.013%, respectively. The structures of all compounds were confirmed by NMR spectroscopy, with ^{1}H and ^{13}C NMR spectral data revealing characteristic functional groups. Although these compounds have previously been reported from *Hericium* species, the present study confirms their occurrence in *H. coralloides* basidiomes cultivated under

Thai environmental conditions. Furthermore, it provides the first quantitative assessment of these bioactive yields from locally sourced and cultivated materials.



(22*E*)-Ergosta-7,9,22-trien-3*β*-ol (**1**)

Ergosterol (**3**)

Hericene A (**2**)

Fig. 3 – Structures of (22*E*)-ergosta-7,9,22-trien-3*β*-ol (**1**), (4-((2*E*)-3,7-dimethyl-2,6-octadien-1-yl)-2-formyl-3-hydroxy-5-methoxyphenyl)methyl hexadecanoate (hericene A) (**2**), and (22*E*)-ergosta-5,7,22-trien-3*β*-ol (ergosterol) (**3**).

Compound **1** was isolated as a white solid powder. Its molecular formula was determined as $C_{28}H_{44}O$ based on the HR-(+) ESI-MS revealing a protonated molecular ion and a sodium adduct at *m/z* 397.348 $[M + H]^+$ and 419.3202 $[M + Na]^+$, respectively. The ^{1}H NMR (500 MHz, $CDCl_3$): δ_H 5.57 (dd, *J* = 5.7, 2.5 Hz, 1H), 5.38 (dt, *J* = 5.5, 2.7 Hz, 1H), 5.25–5.14 (m, 2H), 3.64 (tt, *J* = 11.3, 4.3 Hz, 1H), 2.47 (ddd, *J* = 14.3, 4.8, 2.4 Hz, 1H), 2.28 (ddq, *J* = 14.0, 11.5, 2.3 Hz, 1H), 2.10–1.93 (m, 3H), 1.93–1.82 (m, 4H), 1.60 (s, 5H), 1.54–1.43 (m, 3H), 1.41–1.22 (m, 6H), 1.03 (d, *J* = 6.6 Hz, 3H), 0.94 (s, 3H), 0.92 (d, *J* = 6.8 Hz, 3H), 0.85–0.80 (m, 6H), 0.63 (s, 3H). The ^{13}C NMR (125 MHz, $CDCl_3$): δ_C 141.52, 139.93, 135.72, 132.12, 119.74, 116.43, 70.62, 55.88, 54.71, 46.39, 42.98, 42.97, 40.94, 40.57, 39.23, 38.52, 37.18, 33.24, 32.14, 28.44, 23.14, 21.25, 20.10, 17.75, 16.43, 12.20. Based on these ^{1}H and ^{13}C NMR spectral data, compound **1** was identified as (22*E*)-ergosta-7,9,22-trien-3*β*-ol compared to previously reported data (Chen et al. 2020).

Compound **2** was isolated as a green-brown oil. Its molecular formula was established as $C_{35}H_{56}O_5$ determined based on the HR-(+) ESI-MS revealing a protonated molecular ion peak at *m/z* 555.4064 $[M + H]^-$ indicating eight degrees of unsaturation. The ^{1}H NMR (500 MHz, $CDCl_3$): δ_H 12.36 (d, *J* = 4.1 Hz, 1H), 10.11 (d, *J* = 4.2 Hz, 1H), 6.53 (d, *J* = 4.2 Hz, 1H), 5.41–5.28 (m, 5H), 5.17 (t, *J* = 7.0 Hz, 1H), 5.09–5.03 (m, 1H), 3.92 (d, *J* = 3.8 Hz, 4H), 3.34 (d, *J* = 7.0 Hz, 2H), 2.77 (t, *J* = 6.5 Hz, 1H), 2.34 (t, *J* = 7.5 Hz, 2H), 2.04 (ddt, *J* = 18.0, 13.0, 6.8 Hz, 5H), 1.99–1.90 (m, 2H), 1.77 (d, *J* = 4.4 Hz, 3H), 1.71–1.54 (m, 14H), 1.38–1.20 (m, 31H), 0.92–0.80 (m, 5H). The ^{13}C NMR (125 MHz, $CDCl_3$): δ_C 193.49, 173.63, 173.58, 163.88, 163.29, 138.81, 138.80, 136.16, 131.63, 130.63, 130.42, 130.11, 128.47, 128.30, 124.75, 121.60, 118.48, 113.28, 106.01, 63.38, 56.30, 40.17, 34.64, 34.62, 32.33, 32.30, 31.92, 30.17, 30.10, 30.06, 30.04, 29.97, 29.84, 29.76, 29.75, 29.72, 29.62, 29.53, 29.51, 29.48, 27.62, 27.60, 27.57, 27.55, 27.15, 27.08, 26.06, 26.03, 25.28, 25.25, 23.09, 22.97, 21.76, 18.05, 16.50, 14.52, 14.47. Based on these ^{1}H and ^{13}C NMR spectral data, compound **2** was identified as hericene A compared to previously reported data (Li et al. 2014).

Compound **3** was isolated as a white solid powder. Its molecular formula as $C_{28}H_{44}O$ was determined based on the HR-(+) ESI-MS unravelling a protonated molecular ion and a sodium adduct at *m/z* 397.348 $[M + H]^+$ and 419.3202 $[M + Na]^+$, respectively, indicating seven degrees of unsaturation. The ^1H NMR (500 MHz, $CDCl_3$): δ_H 6.50 (d, *J* = 8.5 Hz, 1H), 6.29 (d, *J* = 8.5 Hz, 0H), 6.24 (d, *J* = 8.5 Hz, 1H), 5.44–5.10 (m, 3H), 4.03–3.90 (m, 1H), 3.86 (s, 3H), 2.17 (s, 18H), 2.15–2.06 (m, 1H), 2.05–1.80 (m, 7H), 1.79–1.66 (m, 2H), 1.66–1.38 (m, 14H), 1.38–1.14 (m, 7H), 1.09 (s, 3H), 1.00 (dd, *J* = 6.6, 2.2 Hz, 3H), 0.94–0.85 (m, 7H), 0.85–0.77 (m, 10H), 0.74 (s, 3H). The ^{13}C NMR (125 MHz, $CDCl_3$): δ_C 207.17, 135.55, 135.34, 132.45, 130.89, 82.30, 79.57, 77.41, 77.16, 76.91, 66.61, 56.34, 51.82, 51.22, 44.70, 42.91, 39.88, 39.48, 37.11, 37.07, 34.83, 33.21, 31.08, 30.26, 28.79, 23.54, 21.02, 20.77, 20.09, 19.78, 18.32, 17.70, 13.01. Based on these ^1H and ^{13}C NMR spectral data, compound **3** was identified as ergosterol, which is consistent with previously published data for ergosterol (Chen et al. 2020).

While the three compounds isolated in our study are known and some are commercially available, our objective was not merely to evaluate their biological activity in isolation, but rather to verify their natural presence, abundance, and bioactivity within cultivated *H. coralloides*. The identification of (22*E*)-ergosta-7,9,22-trien-3*β*-ol (**1**) follows reports of similar ergostane type sterols in fungi (Rivera et al. 2009), hericene A (**2**) has been previously quantified at ~3 mg/g dry weight in *H. erinaceus* (Turk et al. 2021), and ergosterol (**3**) is a major bioactive fungal sterol known for its anticancer properties (Fangkrathok et al. 2013). Moreover, prior studies confirm that chemical profiling of *H. coralloides* includes these metabolites (Wittstein et al. 2016, Narmuratova et al. 2023, Sum et al. 2024).

Effects of compounds isolated from *Hericium coralloides* on cancer cells

All compounds (**1–3**) were initially investigated for their cytotoxicity against three cancer cell lines: A549, Huh-7, and SW-480. These cells were treated with a serial dilution of each compound for 72 h, and cell viability was then assessed using the MTT assay. The results showed that compounds **1**–**3** exhibited varying levels of cytotoxicity on cancer cells (Fig. 4). The IC_{50} values are summarized in Table 4. Among these compounds, ergosterol (**3**) had the strongest cytotoxic activity against A549 (IC_{50} = 4.61 ± 0.04 µg/mL; 11.6 µM), Huh-7 (IC_{50} = 4.267 ± 0.04 µg/mL; 10.6 µM), and SW-480 (IC_{50} = 5.209 ± 0.05 µg/mL; 13.1 µM). Therefore, ergosterol (**3**) exhibited the strongest cytotoxic activity, with IC_{50} values between 4.2–5.6 µg/mL across all cell lines, indicating its potential as a lead compound for anticancer development.

These values are comparable to or slightly stronger than those reported for ergosterol isolated from other medicinal mushrooms (Dulay et al. 2022). Previous studies have reported IC_{50} values ranging from approximately 6–15 µg/mL for ergosterol isolated from *Ganoderma* species and *Lentinus* species against various cancer cell lines (Lee et al. 2011). The relatively low IC_{50} values observed in the present study suggest that ergosterol derived from *Hericium coralloides* may possess considerable anticancer potential. The anticancer activity of ergosterol has been associated with several mechanisms, including the induction of apoptosis, modulation of reactive oxygen species (ROS), and cell cycle arrest in cancer cells (Lee et al. 2011, Li et al. 2015). Ergosterol (**3**) has also been reported to inhibit tumor cell proliferation and migration through the regulation of signaling pathways involved in cell survival and apoptosis (Li et al. 2015).

Table 4 The IC_{50} value of **1**–**3** of *H. coralloides* against various cancer cell lines.

	IC_{50} (µg/mL) value ± SD		
	A549	**Huh-7**	**SW-480**
Compound **1**	16.39 ± 0.06	26.54 ± 0.17	23.87 ± 0.22
Compound **2**	116.60 ± 0.04	50.40 ± 0.07	96.65 ± 0.09
Compound **3**	4.61 ± 0.04	5.209 ± 0.05	4.267 ± 0.04

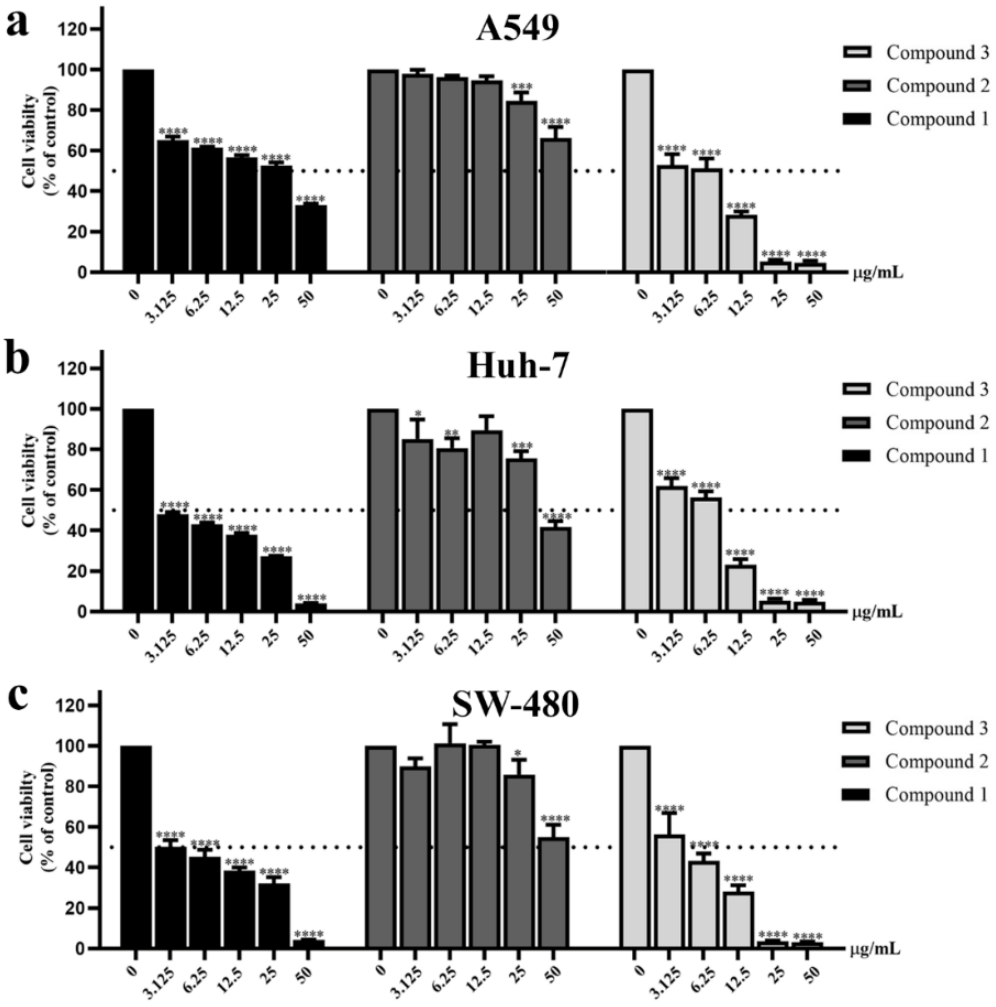


Fig. 4 – Cytotoxicity of compounds **1**–**3** from *H. coralloides* against a A549, b Huh-7 and c SW-480 cells. Bar graphs represent the mean ± SD (n=3). * $p < 0.03$, ** $p < 0.02$, *** $p < 0.002$, **** $p < 0.0001$ vs. untreated control (0 µg/mL).

Effects of ergosterol (3) on colony formation of cancer cells

When a cell detaches from a primary tumor, it typically adheres to a distant site to grow and metastasize. The clonogenic assay is a widely used method to study cell adhesion (Thakor et al. 2017). As shown in Fig. 5, ergosterol (**3**) significantly reduced colony formation in A549, Huh-7, and SW-480 cell lines, at 5 and 10 µg/mL. This suggests that ergosterol (**3**) from *H. coralloides* not only affects cell viability but also inhibits long-term proliferation and survival.

Effect of ergosterol (3) on the migration of cancer cells

The effects of ergosterol (**3**) on the migration ability of cancer cell lines were evaluated using a wound healing-scratch assay. The results demonstrated that ergosterol (**3**) significantly inhibited the migration of A549 and Huh-7 cells. However, no significant effect was observed for SW-480 cells (Fig. 6). These findings suggest that ergosterol (**3**) selectively suppresses the migratory potential of certain cancer cell lines.

In addition, the lack of significant inhibition may also be related to assay sensitivity or the concentration range tested in the present study (Liang et al. 2007). Similar variations in the response of different cancer cell lines to natural compounds have been reported in previous studies, highlighting the importance of cell line–specific factors in determining the effectiveness of anticancer agents (Atanasov et al. 2015).

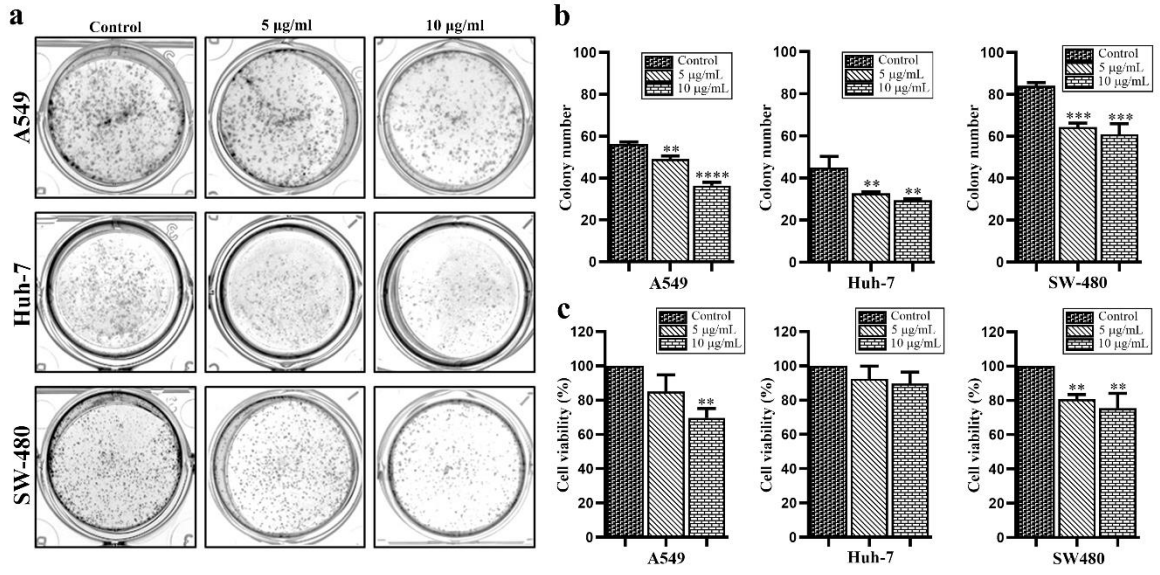


Fig. 5 – Effects of ergosterol (**3**) on colony formation of cancer cells. (a) Representative images of the formed colonies of A549, Huh7, and SW-480 cells after treatment with varying concentrations of ergosterol (**3**). (b) Number of formed colonies and (c) cell viability of A549, Huh7, and SW-480 cells after a 7-day culture period. Bar graphs represent the mean ± SD (n=3). * $p < 0.03$, ** $p < 0.02$, *** $p < 0.002$, **** $p < 0.0001$ vs. untreated control (0 µg/mL).

Currently, cancer is a worldwide public health problem and is the second leading cause of death (Bray et al. 2024). In 2022, approximately 1.8 million cancer-related deaths were attributed to lung cancer (18.7%), followed by colorectal cancer (9.3%) and liver cancer (7.8%) (Bray et al. 2024). Several natural substances from both terrestrial and marine sources have demonstrated significant anticancer properties. Rangsinth (2023) reported that ergosterol possesses various pharmacological properties, including anticancer activity.

Ergosterol (**3**) demonstrated potential anticancer properties across various cancer types by inhibiting proliferation, inducing apoptosis, and modulating key signaling pathways. In bladder cancer, it suppresses androgen signalling and inflammation-related pathways (Ikarashi et al. 2020, Yazawa et al. 2020). For breast cancer, it reduces ROS, DNA damage, and ERK activation, triggers S-phase cell cycle arrest, and promotes apoptosis (Pluchino et al. 2015, Chen et al. 2017). It also inhibits proliferation in oesophageal (Lin et al. 2022), gastric (Lin et al. 2022), liver (Chen et al. 2017), lung (Lin et al. 2022), and prostate cancers by affecting cell viability and androgen receptors (Muñoz-Fonseca et al. 2021). Additionally, ergosterol (**3**) enhances ROS levels in liver cancer when combined with amphotericin B (Chen et al. 2017) and exhibits anti-angiogenic properties in tumor models (Chen et al. 2017).

However, the effects of bioactive compounds in *H. coralloides* on cancer cells remain under investigation. Wittstein et al. (2016) reported that corallocins A−C, a class of terpenoids, featuring an isoindolinone structure, have varying levels of antiproliferative activity. Among them, only corallocin B exhibited antiproliferative activity against MCF-7 (breast cancer), KB-3-1 (cervical cancer), and HUVEC (human umbilical vein endothelial) cell lines. In contrast, Sum et al. (2024) found that corallocins D−E showed no significant effect on the proliferation of A431 (epidermoid carcinoma), SKOV-3 (ovarian cancer), PC3 (prostate cancer), and A549 (lung cancer) cell lines.

In this study, hericene A (**2**) and ergosterol (**3**) from *H. coralloides* demonstrated stronger antiproliferative activity against A549 cells compared to those reported by Sum et al. (2024), as well as Huh-7 (liver cancer) and SW-480 (colorectal cancer) cells. In addition, ergosterol (**3**) showed potent antiproliferative activity against A549 cells, with an IC_{50} value of 4.6 µg/mL (11.60 µM), which is more effective than the findings of Lin and his fellow team (Lin et al. 2022), who

reported an IC_{50} of 42.22 µM. Notably, ergosterol (**3**) also reduced colony formation and inhibited migration of A549, Huh-7, and SW-480 cells, suggesting the therapeutic potential of *H. coralloides* and its bioactive compounds, particularly ergosterol (**3**) in cancer treatment.

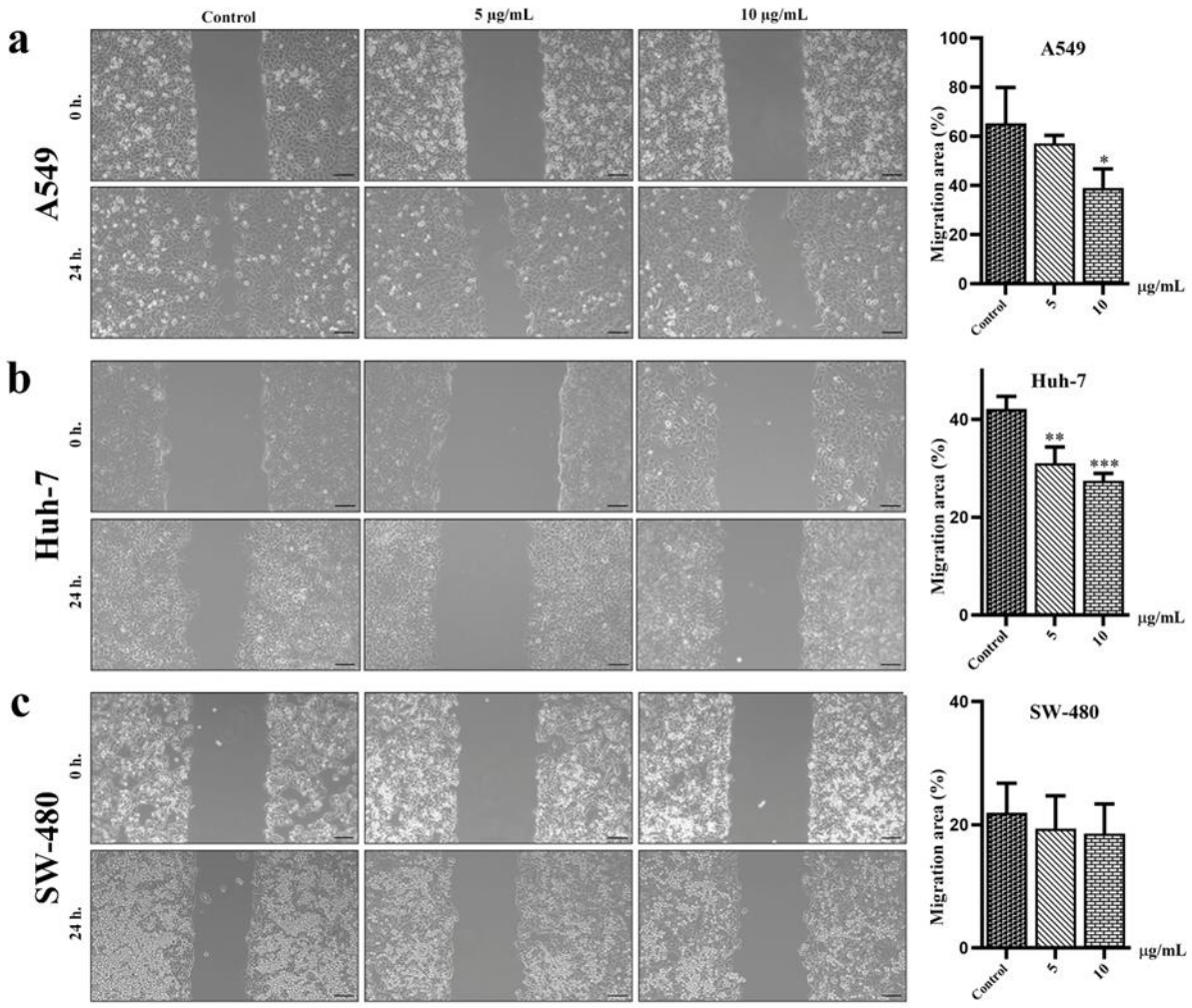


Fig. 6 – Effect of ergosterol (**3**) on the migration of cancer cells. Representative images of the wound area at 0 hours and 24 hours post-scratching, along with the percentage of migration area for (a) A549, (b) Huh-7, and (c) SW-480 cells after treatment with varying concentrations of ergosterol (3). Scale bar = 100 µm. Bar graphs represent the mean ± SD (n=3). * $p < 0.03$, ** $p < 0.02$, *** $p < 0.002$, **** $p < 0.0001$ vs. untreated control (0 µg/mL).

In addition, all three compounds exhibit minimal toxicity toward normal mammalian cell lines or immune cells at typical concentrations. A previous study showed that ergosterol exhibited an $IC_{50} > 100$ µM in normal cell lines, indicating low cytotoxicity at doses effective in cancer models (Rangsinth et al. 2023). (22*E*)-Ergosta-7,9,22-trien-3*β*-ol (**1**) and ergosterol (**3**) exhibit low to no cytotoxicity in human normal cell lines at concentrations effective in cancer cells (Huang et al. 2021); quantitative toxicity data for hericene A (**2**) are currently limited.

A limitation of the present study is the absence of a standard chemotherapeutic drug as a positive control in the MTT, clonogenic, and migration assays (Franken et al. 2006). In many anticancer studies, drugs such as doxorubicin are commonly used as reference compounds (Thorn et al. 2011). Previous reports indicate that doxorubicin exhibits IC_{50} values in the low micromolar range against A549, SW-480, and Huh-7 cell lines (Minotti et al. 2004). Although a direct comparison cannot be made in the present study, the relatively low IC_{50} values observed for ergosterol indicate notable cytotoxic activity. In comparison, the doxorubicin had IC_{50} values that varied with assay conditions around 2.2 µM at 12 h exposure (Maryam et al. 2017), and around

70 µM (0.07 mM) after 72 h in A549 lung cancer cells (Kashkin et al. 2010). This places higher doxorubicin's potency than ergosterol (**3**). Although IC_{50} values for doxorubicin in SW-480 colorectal cancer are not directly reported, they are generally within micromolar range. Future studies should include established chemotherapeutic agents as positive controls to enable a more comprehensive evaluation of the anticancer potency of compounds isolated from *Hericium coralloides*.

Despite the promising findings, several limitations should be acknowledged. The anticancer activity of ergosterol (**3**) was evaluated only using *in vitro* cell-based assays, and further validation using *in vivo* models is required to confirm its therapeutic potential. Standard chemotherapeutic drugs were not included as positive controls in the bioassays, which limits direct comparison of cytotoxic potency. In addition, the molecular mechanisms underlying the observed anticancer activity were not investigated in this study. Future research should focus on elucidating the signaling pathways involved in ergosterol-mediated cytotoxicity, as well as evaluating its efficacy in animal models and exploring potential synergistic effects with existing anticancer drugs.

Conclusions

This study presents the first successful cultivation of *H. coralloides* in Thailand, achieving mature fruiting bodies across three substrate treatments with no statistically significant differences in yield. While all treatments supported growth effectively, substrate treatment 1, comprising para-rubber sawdust supplemented with rice bran and sugar, proved to be the most cost-effective option. Therefore, it is recommended as the preferred substrate for the cultivation of *H. coralloides* under similar conditions. Nutritional analysis confirmed *H. coralloides* as a rich source of carbohydrates, protein, and crude fibers. Ergosterol (**3**) from the fruiting body extract exhibits strong anticancer effects by reducing colony formation and inhibiting migration on A549, Huh-7, and SW-480 cell lines. These findings highlight the potential of *H. coralloides* for applications in food and nutraceutical products. Further research is needed to elucidate the mechanism of action of ergosterol (**3**) and its therapeutic potential for cancer treatment.

Acknowledgements

This work was supported by a grant from Research and researcher for industries (Grant No. PHD62I0018/2562), and funding from the grant "Sustainable development of knowledge on fungi for future utilization (Grant No. 682A16033)" by Mae Fah Luang University has received funding support from the National Science, Research and Innovation Fund (NSRF) via Fundamental fund (FF). The authors also acknowledge Mae Fah Luang University, and the Institute of Medicinal Plant Innovation Center of Mae Fah Luang University for providing the necessary research facilities. The Alexander von Humboldt (AvH) foundation is gratefully acknowledged for supporting S.S.E. through the Georg-Forster Fellowship for Experienced Researchers stipend (Ref 3.4-1222288-EGY-GF-E).

References

Aluksanasuwan S, Somsuan K, Ngoenkam J, Chiangjong W, et al. 2024 – Knockdown of heat shock protein family D member 1 (HSPD1) in lung cancer cell altered secretome profile and cancer-associated fibroblast induction. Biochimica et Biophysica Acta (BBA)-Molecular Cell Research 1871(5), 119736.

AOAC. 2019 – Official Methods of Analysis of the Association of Official Analytical Chemists: Official Methods of Analysis of AOAC International. 21st Edition, Association of Official Analytical Chemist International, Washington DC.

AOAC. 2023 – Official Methods of Analysis of the Association of Official Analytical Chemists: Official Methods of Analysis of AOAC International. 22nd Edition, Oxford University Press.

Atila F, Tüzel Y, Pekşen A, Cano AF, Fernández JA. 2021 – The effect of different fruiting temperatures on the yield and nutritional parameters of some wild and hybrid *Hericium* isolates. Scientia Horticulturae 280, 109915.

Atanasov AG, Waltenberger B, Pferschy-Wenzig EM, Linder T, et al. 2015 – Discovery and resupply of pharmacologically active plant-derived natural products: A review. Biotechnology advances 33(8), 1582–1614.

Bray F, Laversanne M, Sung H, Ferlay J, et al. 2024 – Global cancer statistics 2022: GLOBOCAN estimates of incidence and mortality worldwide for 36 cancers in 185 countries. CA: A Cancer Journal for Clinicians 74(3), 229−263.

Chen S, Yong T, Zhang Y, Su J, et al. 2017 – Anti-tumor and anti-angiogenic ergosterols from *Ganoderma lucidum*. Frontiers in Chemistry 5, 85.

Chen Z, Yuan X, Buchanan P, Quek SY. 2020 – Isolation and determination of lipophilic mycochemicals from a New Zealand edible native mushroom *Hericium novae-zealandiae*. Journal of Food Composition and Analysis 88, 103456.

Demirtas N, Sengul GF, Dizeci N, Yildirim O. 2024 – Exploring the chemical composition and nutritional properties of six edible mushroom species from Turkey. Journal of Food Composition and Analysis 133, 106477.

Dulay RMR, Cabrera EC, Kalaw SP, Reyes RG, et al. 2022 – Cytotoxicity of *Lentinus* isolates mycelial extracts on human colorectal carcinoma HCT-116 cells. Journal of Applied Pharmaceutical Science 12(6), 076–085.

Fangkrathok N, Sripanidkulchai B, Umehara K, Noguchi H. 2013 – Bioactive ergostanoids and a new polyhydroxyoctane from *Lentinus polychrous* mycelia and their inhibitory effects on E2-enhanced cell proliferation of T47D cells. Natural Product Research 27(18), 1611−1619.

FAO. 2023 – Food Energy—Methods of Analysis and Conversion Factors. Food and Agriculture Organization Food and Nutrition Paper No. 77.

Franken NA, Rodermond HM, Stap J, Haveman J, Van Bree C. 2006 – Clonogenic assay of cells *in vitro*. Nature protocols 1(5), 2315–2319.

Grimm D, Wösten HA. 2018 – Mushroom cultivation in the circular economy. Applied Microbiology and Biotechnology 102(18), 7795–7803.

Gonkhom D, Luangharn T, Stadler M, Thongklang N. 2024 – Cultivation and nutrient compositions of medicinal mushroom, *Hericium erinaceus* in Thailand. Chiang Mai Journal of Science 51(2), 1−10.

Guan Y, Shi D, Wang S, Sun Y, et al. 2023 – *Hericium coralloides* ameliorates Alzheimer's disease pathologies and cognitive disorders by activating Nrf2 signaling and regulating gut microbiota. Nutrients 15(17), 3799.

Heleno SA, Barros L, Martins A, Queiroz MJR, et al. 2015 – Chemical composition, antioxidant activity and bioaccessibility studies in phenolic extracts of two *Hericium* wild edible species. LWT-Food Science and Technology 63(1), 475−481.

Huang YP, Chen DR, Lin WJ, Lin YH, et al. 2021 – Ergosta-7,9(11),22-trien-3β-ol attenuates inflammatory responses via inhibiting MAPK/AP-1 induced IL-6/JAK/STAT pathways and activating Nrf2/HO-1 signaling in LPS-stimulated macrophage-like cells. Antioxidants 10(9), 1430.

Ikarashi N, Hoshino M, Ono T, Toda T, et al. 2020 – A mechanism by which ergosterol inhibits the promotion of bladder carcinogenesis in rats. Biomedicines 8(7), 180.

Index Fungorum. 2025 – http://www.indexfungorum.org/. (Accessed on January 10, 2025).

Jianzhao QI, Jing WU, Shijie KANG, Jingming GAO, et al. 2024 – The chemical structures, biosynthesis, and biological activities of secondary metabolites from the culinary-medicinal mushrooms of the genus *Hericium*: a review. Chinese Journal of Natural Medicines 22(8), 676−698.

Kashkin KN, Musatkina EA, Komelkov AV, Favorskaya IA, et al. 2010 – Expression profiling and putative mechanisms of resistance to doxorubicin of human lung cancer cells. Doklady. Biochemistry and Biophysics 430(1), 20–23.

Kim JY, Woo EE, Lee IK. 2018 – New antioxidants from the culture broth of *Hericium coralloides*. The Journal of Antibiotics 71(9), 822−825.
Ko HG, Park HG, Park SH, Choi CW, et al. 2005 – Comparative study of mycelial growth and basidiomata formation in seven different species of the edible mushroom genus *Hericium*. Bioresource Technology 96(13), 1439−1444.
Koga J. 2024 – A multilocus phylogeny of *Hericium* fungi in Canada and their production of erinacine A (Master's thesis, The University of Western Ontario (Canada).
Kuo M. 2020 – *Hericium coralloides*. Retrieved from the MushroomExpert.Com Web site: http://www.mushroomexpert.com/hericium_coralloides.html. Accessed 10 January 2025
Lazur J, Kała K, Krakowska A, Sułkowska-Ziaja K, et al. 2024 – Analysis of bioactive substances and essential elements of mycelia and fruiting bodies of *Hericium* spp. Journal of Food Composition and Analysis 127, 105981.
Lee MK, Hung TM, Cuong TD, Na M, et al. 2011 – Ergosta-7,22-diene-2*β*,3*α*,9*α*-triol from the fruit bodies of *Ganoderma lucidum* induces apoptosis in human myelocytic HL-60 Cells. Phytotherapy Research 25(11), 1579−1585.
Li W, Sun YN, Zhou W, Shim SH, Kim YH. 2014 – Erinacene D, a new aromatic compound from *Hericium erinaceum*. The Journal of Antibiotics 67(10), 727−729.
Li X, Wu Q, Xie Y, Ding Y, et al. 2015 – Ergosterol purified from medicinal mushroom *Amauroderma* rude inhibits cancer growth *in vitro* and *in vivo* by up-regulating multiple tumor suppressors. Oncotarget 6(19), 17832.
Liang CC, Park AY, Guan JL. 2007 − *In vitro* scratch assay: a convenient and inexpensive method for analysis of cell migration *in vitro*. Nature protocols 2(2), 329−333.
Lin Y, Wen B, Zhang Z, Cai J. 2022 – Ergosterol peroxide: An effect-directed detecting method from *Anoectochilus elwesii* and evaluation of anticancer activity. Natural Product Research 36(12), 3177−3182.
Maryam A, Mehmood T, Zhang H, Li Y, et al. 2017 – Alantolactone induces apoptosis, promotes STAT3 glutathionylation and enhances chemosensitivity of A549 lung adenocarcinoma cells to doxorubicin via oxidative stress. Scientific Reports 7(1), 6242.
Miles PG, Chang ST. 2004 – Mushrooms: cultivation, nutritional value, medicinal effect, and environmental impact. CRC press.
Minotti G, Menna P, Salvatorelli E, Cairo G, et al. 2004 – Anthracyclines: molecular advances and pharmacologic developments in antitumor activity and cardiotoxicity. Pharmacological Reviews 56(2), 185–229.
Morchang A, Somsuan K, Rongjumnong A, Weeraphan C, et al. 2025 – Proteomic analysis reveals a potential anticancer mechanism for a novel effervescent curcumin-ascorbic acid-polysaccharide-*β*-cyclodextrin inclusion complex towards colorectal cancer cells through modulation of ribosome biogenesis. Carbohydrate Polymer Technologies and Applications 10, 100775.
Muñoz-Fonseca MB, Vidal-Limon A, Fernández-Pomares C, Rojas-Durán F, et al. 2021 – Ergosterol exerts a differential effect on AR-dependent LNCaP and AR-independent DU-145 cancer cells. Natural Product Research 35, 4857–4860.
Narmuratova Z, Bisko N, Mustafin K, Al-Maali G, et al. 2023 – Screening of medicinal mushroom strains with antimicrobial activity and polysaccharides production. Turkish Journal of Biochemistry 48(3), 290−297.
Pasailiuk MV, Sukhomlyn MM, Gryganskyi AP. 2019 – Patterns of *Hericium coralloides* growth with competitive fungi. Czech Mycology 71(1), 49−63.
Pewlong W, Sajjabut S, Chookaew S, Eamsiri J. 2019 – Effects of gamma irradiation on microbial load and chemical properties for preserve dried shiitake mushroom powder. CMUJ NS Special Issue on Food and Applied Bioscience to Innovation and Technology 18(2), 1−12.
Pluchino LA, Liu AK, Wang HC. 2015 – Reactive oxygen species-mediated breast cell carcinogenesis enhanced by multiple carcinogens and intervened by dietary ergosterol and mimosine. Free Radical Biology and Medicine 80, 12–26.

Qi J, Liu Y, Wu J, Kawagishi H, Liu C. 2025 – Bibliometric analysis of *Hericium* mushrooms for medicinal and food purposes: 1992−2023. Journal of Future Foods 5(4), 317−330.

Rangsinth P, Sharika R, Pattarachotanant N, Duangjan C, et al. 2023 – Potential beneficial effects and pharmacological properties of ergosterol, a common bioactive compound in edible mushrooms. Foods 12(13), 2529.

Rivera A, Benavides OL, Rios-Motta J. 2009 – (22*E*)-Ergosta-6,22-diene-3*β*,5*α*,8*α*-triol: A new polyhydroxysterol isolated from *Lentinus edodes* (Shiitake). Natural Product Research (3), 293−300.

Sinclair JB, Dhingra OD. 2017 – Basic plant pathology methods. CRC press.

Sholyavei S, Mishra SK, Panda S. 2020 – Characterization of sporophores, spore Prints, spines, basidia, and basidiospores of seven genotypes of *Hericium erinaceus* (Bull.: Fr.) Pers. Indian Journal of Pure & Applied Biosciences 8(6), 375−383.

Shrivastava A, Jain S. 2024 – *Hericium erinaceus* (Bull.) and *Hericium coralloides*. In: Edible and Medicinal Mushrooms of the Himalayas, CRC Press, 111−127

Somsuan K, Rongjumnong A, Morchang A, Hankittichai P, et al. 2025 – Heat shock protein family D member 1 mediates lung cancer cell induced angiogenesis of endothelial cells. Biomedical Reports 22(5), 77.

Sostherb. 2023 – What is *Hericium* mushroom good for? Knowledge. Xi'an Sost Biotech Co., Ltd. Retrieved August 28, 2025, from https://www.sostherb.com/info/what-is-hericium-mushroom-good-for-88684803.html

Stamets. P 2011 – Growing Gourmet and Medicinal Mushrooms, 3rd Edn., Ten Speed Press.

Suarez-Arnedo A, Figueroa FT, Clavijo C, Arbeláez P, et al. 2020 – An image J plugin for the high throughput image analysis of *in vitro* scratch wound healing assays. Public Library of Science ONE 15(7), e023256.

Sullivan DM, Donald EC. 1993 – Methods of Analysis for Nutrition Labeling, AOAC (Association of Official Analytical Chemist.). International.

Sum WC, Gonkhom D, Ibrahim MA, Stadler M, Ebada SS. 2024 – New isoindolinone derivatives isolated from the fruiting bodies of the basidiomycete *Hericium coralloides*. Mycological Progress 23(1), 4.

Thakor P, Song W, Subramanian RB, Thakkar VR, et al. 2017 – Maslinic acid inhibits proliferation of renal cell carcinoma cell lines and suppresses angiogenesis of endothelial cells. Journal of Kidney Cancer and VHL 4(1), 16.

Thorn CF, Oshiro C, Marsh S, Hernandez-Boussard T, et al. 2011 – Doxorubicin pathways: pharmacodynamics and adverse effects. Pharmacogenetics and Genomics 21(7), 440–446.

Thongbai B, Wittstein K, Richter C, Miller SL, et al. 2017 – Successful cultivation of a valuable wild strain of *Lepista sordida* from Thailand. Mycological Progress 16(4), 311−323.

Turk A, Yeon SW, Ryu SH, Ko SM, et al. 2021 – Effect of culture conditions on the content of hericene A, an *α*-glucosidase inhibitory constituent of *Hericium erinaceus*. Scientia Horticulturae 288, 110407.

Van der Merwe B, Herrmann P, Jacobs K. 2023 – *Hericium ophelieae* sp. nov., a novel species of *Hericium* (Basidiomycota: Russulales, Hericiaceae) from the Southern Afrotemperate forests of South Africa. Mycology 14(2), 133−141.

Williams LM, Berthon BS, Stoodley IL, Williams EJ, Wood LG. 2023 – Medicinal mushroom extracts from *Hericium coralloides* and *Trametes versicolor* exert differential immunomodulatory effects on immune cells from older adults *in vitro*. Nutrients 15(9), 2227.

Wiraswati HL, Ma'ruf IF, Sharifi-Rad J, Calina D. 2025 – Piperine: an emerging biofactor with anticancer efficacy and therapeutic potential. BioFactors 51(1), 2134.

Wittstein K, Rascher M, Rupcic Z, Löwen E, et al. 2016 – Corallocins A–C, nerve growth and brainderived neurotrophic factor inducing metabolites from the mushroom *Hericium coralloides*. Journal of Natural Products 79, 2264–2269.

Yazawa Y, Ikarashi N, Hoshino M, Kikkawa H, et al. 2020 – Inhibitory effect of ergosterol on bladder carcinogenesis is due to androgen signaling inhibition by brassicasterol, a metabolite of ergosterol. Journal of Natural Medicines 74, 680–688.

Zhang J, Zhang J, Zhao L, Shui X, et al. 2019 – Antioxidant and anti-aging activities of ethyl acetate extract of the coral tooth mushroom, *Hericium coralloides* (Agaricomycetes). International Journal of Medicinal Mushrooms 21(6), 561−570.

Zhang ZF, Lv GY, Song TT, Xu ZW, Wang MY. 2024 – Effects of different extraction methods on the structural and biological properties of *Hericium coralloides* polysaccharides. Food Chemistry 445, 138752.

Zhu Y, Jia C, Wang C, Zhang S, et al. 2024 – Yield increment and transcriptome response caused by blue light treatment in *Hericium coralloides*. BMC Genomics 25(1), 1244.

Supplementary materials

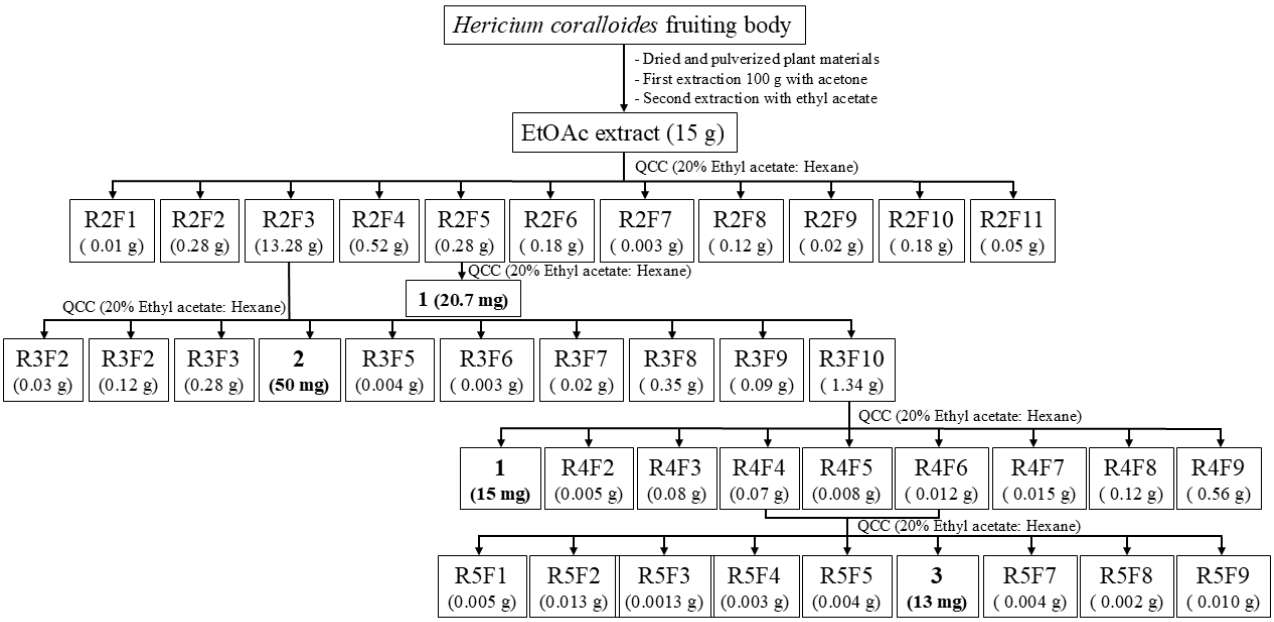


Figure S1 – Schematic diagram of the extraction and isolation of compounds **1**−**3** from the fruiting body of *Hericium coralloides*.